Design and Wind Tunnel Study of a Top-mounted Diverterless Inlet

TAN Hui-jun, GUO Rong-wei
(Internal Flow Research Center, Nanjing University of Aeronautics and Astronautics, Nanjing 210016, China)

Abstract: Combined with a UAV of the shape like Global Hawk, a new inlet is advanced to obtain high performance in both Radar Cross Section(RCS) and aerodynamic drag. Efforts are made to achieve this goal such as adopting a top-mounted inlet configuration, utilizing the diverterless technique and putting forward a new shape of entrance. A design method is brought forward and verified by wind tunnel tests. Results indicate: (1) Despite the negative effect of the front fuselage and the absence of the conventional boundary diverter, the performance of the top-mounted diverterless inlet advanced here (Ma: 0.50-0.70, α: $-4°$-$6°$, $\sigma > 0.975$) is equivalent to that of conventional S shaped inlet with diverter; (2) The integration of the inlet with the fuselage is realized by the utilization of a special inlet section and the diverterless technique, which disposes the whole inlet in the shield of the head of UAV, improving the drag characteristics and the stealthy performance of the aircraft; (3) The bump which is equal to the local boundary layer thickness in height can divert the boundary layer effectively. As a result, no obvious low total pressure zone is found at the outlet of the inlet; (4) According to the experimental results, negative angle of attack is favorable to the total pressure recovery and positive angle of attack is favorable to the total pressure distortion, while yaw brings bad effects on both; (5) The design of cowl lip is of great importance to the inlet performance at yaw, therefore, further improvement of the inlet performance will rely on the lip shapes of the cowl chosen.

Key words: top-mounted inlet; diverterless inlet; unmanned air vehicle; design; wind tunnel test
一种无人机用背负式无附面层隔道进气道的设计及实验验证. 谭慧俊, 郭荣伟. 中国航空学报(英文版), 2004, 17(2): 72-78.

摘 要: 结合一类似于"全球鹰"的无人侦察机外形, 对一种新型高隐身低外阻进气道进行了如下设计: 采用背负式布局方案, 使用无隔道技术, 并提出了一种新的进口截面形状。加工了风洞试验模型并开展了验证性风洞实验研究工作。结果表明: (1) 尽管受到机头遮蔽的不利影响, 且没有采用传统的附面层隔道, 所给出的背负式无隔道进气道方案性能(Ma: 0.50~0.70, α: $-4°$~$6°$, $\sigma > 0.975$)与常规的有隔道"S"弯进气道相当; (2) 特殊进口截面形状及无附面层隔道技术的采用将进气道与机身有机地融为一体, 使进气道整体都处于飞行器头部的遮蔽之中, 这有利于改善飞行器的阻力特性和隐身性能; (3) 进气道出口截面上未发现因附面层吸入而造成的低总压区, 这说明高度与当地附面层厚度相当的进口鼓包能有效地隔除附面层中能量较低的气流; (4) 研究范围内, 负攻角对进气道的总压恢复系数有利, 正攻角对周向畸变指数有利, 而侧滑角则对两者均有着不利影响; (5) 唇口的设计对进气道的侧滑角性能有着重要影响, 进气道性能的进一步提高应考虑唇口设计的改进。

关键词: 背负式进气道; 无隔道进气道; 进气道; 无人机; 设计; 实验
文章编号: 1000-9361(2004)02-0072-07 中图分类号: V211.3 文献标识码: A

Top-mounted inlets have advantages over conventional inlet configurations as leaving more space underneath to place missiles or other weapons, providing better environments for ground crew, increasing stealthy capabilities to up-looking radar, and preventing foreign objects from ingesting into engines[1]. They are quite common on commercial aircrafts when three engines are desired like on the

Received date: 2003-05-19; Revision received date: 2004-02-10

McDonald Douglas DC-10, MD-11. However, the complex aerodynamics issues, especially at high angles of attack, impeding the top-mounted inlets' wide use on military aircrafts, and at present they are mainly applied to UCAVs and bombers such as Global Hawk, X-45, X-47 and B-2.

In the fifties of last century, the explorations of the diverterless technique were initiated by researchers in NACA Lewis Laboratory[2]. But the diverterless technique did not get further attentions until its recent successful application in X-35. This unique technique, eliminating the diverter and other features associated with boundary layer management, is realized by designing a three-dimensional surface, or bump, front of the inlet aperture, which can decelerate part of the coming flow and create a pressure gradient that pushes the boundary layer away from the inlet. Thus, this technique is able to reduce the overall weight of the aircraft, cut down the frontal area of the aircraft[3], improve the drag characteristics and enhance the stealthy capabilities by decreasing corner reflections of radar waves.

According to domestic open literature, little work has been made on the top-mounted inlet or the diverterless technique, let alone the combination of both. Integrated with a UAV of the configuration like Global Hawk, a top-mounted S shaped inlet utilizing the diverterless technique is devised and verified by wind tunnel tests in this study.

1 Description of the Forebody

Fig. 1 demonstrates the forepart of an aircraft, which resembles the Global Hawk, the UAV of US Air Force. The distance from the apex of the fuselage to the leading edge of the inlet is L. As shown in the figure, a bulge which is $0.06L$ in height rests on the top side of the fuselage. Because the wings are below and far away from the inlet, it is obvious that they have little influence on the performance of the inlet at low incidence. Accordingly the design and wind tunnel tests of the inlet in this paper have not taken the effect of the wings into account.

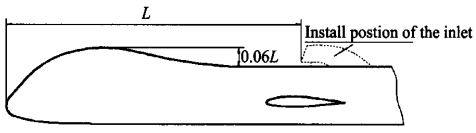

Fig. 1 Sketch of the fuselage

2 Design of the Inlet

The bulge at the front fuselage shadows the top-mounted inlet and is believed to reduce the frontal aspect Radar Cross Section (RCS) of the inlet. However, it is a great challenge to design the inlet because the bulge speeds up the development of the boundary layer, resulting in the aperture of the inlet mostly in the boundary layer. In order to solve the problem mentioned, the Global Hawk adopts higher boundary diverter, which lifts the inlet to ameliorate the flow condition in front of the aperture. But this approach will increase RCS and the aerodynamic drag of the aircraft. Hence, a top-mounted inlet integrated with the fuselage is brought forward to dispose the whole inlet in the shield of the bulge. The diverterless technique is utilized in this design to deal with the thick boundary flow and to obtain better conformance. Additional endeavours are also made to acquire favorable inlet performance.

Though the conventional design method[4] of S shaped inlet is still used here, a creative cross section is come up with, which conveniently integrate the inlet with the fuselage and the bump employed by the diverterless technique. The procedure of the inlet design is described in detail in the following.

2.1 General geometrical parameters of the inlet

For some general parameters of the inlet such as length, offset and exit area are subject to geometric constraints of the fuselage and the engine, they are always known when one set out to design a inlet. According to a selected area ratio, the entrance area of the inlet can then be decided. The parameters used in this paper are summarized in Table 1, two of which are normalized by the diameter of the exit.

Table 1 General geometrical parameters of the inlet

Length/Diameter	Offset/Diameter	Area ratio	Equivalent angle/(°)
5.0	1.6	1.3	1.5

2.2 Design of the entrance shape

The reason why the conventional cross sections like ellipse or raceway shape can not be used here is that the diverterless technique requires the integration of the entrance section with the bump, while neither of these can satisfy this requirement. The newly devised cross section is pictured in Fig. 2, which consists of a cirque (centre angle θ, internal radius r and external radius $r+a+b$) and four quarter-ellipses (major axis a or b and minor axis c). For this configuration there are two merits, one is that it can be integrated with the bump and transformed to the shape of the engine face easily, and the other is that it unites the inlet with the fuselage to the utmost degree achieving low aerodynamic drag and low observability.

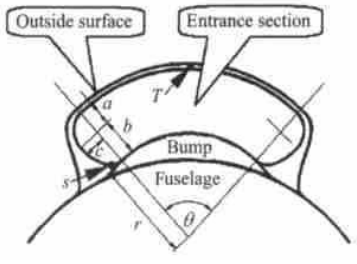

Fig. 2 Sketch of the entrance section

2.3 Centerline and area distributions

The centerline and the area distributions are of great significance to the performance of the inlet. Centerline shapes determine the turning of the internal flow and thereby decide the transverse pressure gradient and the secondary flow in the duct. Area distributions determine the diffusivity and hence control the streamwise pressure gradient imposed on the flow. Inappropriate centerline shape or area distribution may both lead to flow separation. Ref. [4] provides three polynomial functions which are suitable for both centerline shape and area distribution. Based upon previous investigations, the centerline distribution with a modest turning and the area distribution with a rapid change near the exit are used in this study.

2.4 Design of the diffuser

The cross-sectional area (A_i) at arbitrary station of the diffuser can be obtained by its entrance area, exit area and area distribution. Referring to Fig. 2, it is not difficult to deduce the mathematical expression of any cross-sectional area

$$A_i = \frac{\pi a_i c_i}{2} + \frac{\pi b_i c_i}{2} + \frac{\theta_i}{360}\pi(r_i + a_i + b_i)^2 - \frac{\theta_i}{360}\pi r_i^2 \quad (1)$$

Letting $k_{1,i} = \frac{a_i}{c_i}$, $k_{2,i} = \frac{b_i}{c_i}$, $k_{3,i} = \frac{r_i}{c_i}$ and assuming these ratios and θ_i are known, Eq. (1) can be rewritten as

$$c_i = \sqrt{\frac{A_i}{M}} \qquad M = \pi\left[\frac{k_{1,i} + k_{2,i}}{2} + \frac{\theta_i}{360}(k_{1,i} + k_{2,i} + k_{3,i})^2 - \frac{\theta_i}{360}k_{3,i}^2\right]$$

which means that the configuration of this section is exactly determined. $k_{1,i}$, $k_{2,i}$, $k_{3,i}$ and θ_i vary smoothly and monotonously from $k_{1,in}$, $k_{2,in}$, $k_{3,in}$ and θ_{in} to $k_{1,out}$, $k_{2,out}$, $k_{3,out}$ and θ_{out} when the station moves from the entrance to the exit. The values of $k_{1,in}$, $k_{2,in}$, $k_{3,in}$ and θ_{in} determine the shape of the entrance section, which are selected 1.0, 2.5, 2.5 and 110° individually in this study. While determining $k_{1,out}$, $k_{2,out}$, $k_{3,out}$ and θ_{out} one should be more careful to guaranttee that the exit of the diffuser is an exact circle. The values of 1.0, 1.0, 4.0 and 0° are capable to meet the requirement well and are used here. Result shows that the boundary conditions of $k_{1,i}$, $k_{2,i}$, $k_{3,i}$ and θ_i work well (Fig. 3).

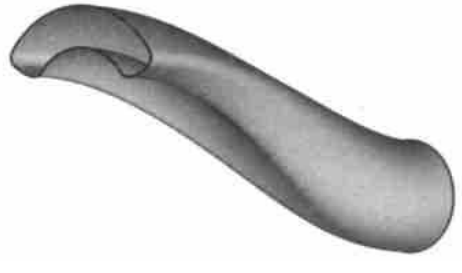

Fig. 3 3-D view of the diffuser

2.5 Design of the bump

The success of the diverterless technique will be largely dependent on the design of the bump. A well designed bump should exert its functions of

both guiding and pushing to keep the boundary layer away from the inlet by elaborate surface design. The effect of guiding depends directly on the bump itself and operates on the lower part of the boundary layer flow. But the effect of pushing appears not so direct and is determined by the pressure gradient formed by the bump acting on the upper layer. With a crescent-shaped cross section and a polynomial vertical section line, the bump is approximate to a cone-shaped surface, which is tangent to the fuselage and the inlet at its boundaries. Computational results indicate that better performance of the inlet can be achieved by a bump of which the maximum height is equivalent to the thickness of the local boundary layer (evaluated by turbulent boundary layer of flat plate) and the length is about five times the maximum height.

2.6 Design of cowl lips

In general, lips of subsonic inlets are of importance to the performance of the inlet. And, withal, in this paper it acts as an additional measure assisting the bump to push boundary flow away from the inlet. A lip scheme with variable section line and variable length is adopted. NACA 1-85-100 lip[5] is at top point of the entrance (T point in Fig. 2) forming a local 'diffuser' (Fig. 4) to acquire higher pressure in region A than that of the outside. Symmetry airfoil is at the intersection point with the bump (S point in Fig. 2) to prevent performance deterioration at yaw. The utilization of variable length lip gets a forward swept cowl which cooperates with the local 'diffuser' and ensures the majority of the boundary layer flow spilling out at the aft notch.

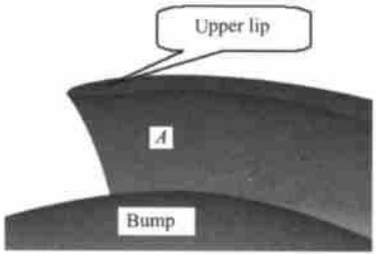

Fig. 4 Feature of the upper lip and the inlet bump

Fig. 5 gives an enlarged view of the inlet's forepart. In virtue of the diverterless technique and the innovative cross section of the inlet, an integration of the inlet and the fuselage is obtained which minimizes the inlet's height and thereby brings the whole inlet into the shadow of the bulge of the fuselage.

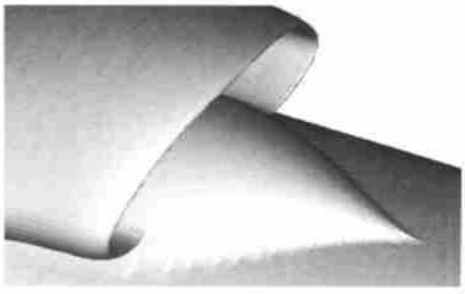

Fig. 5 Enlarged view of the inlet's forepart

In addition, the junction of the inlet and the engine (with center body) is designed using constant area distribution. At the same time, the design of outside surface of the inlet is also conducted.

3 Experimental Verification

In order to obtain the aerodynamic performance of the newly designed inlet and verify the design approach, an experimental inlet model is designed and manufactured and then tested in a wind tunnel.

3.1 Inlet model and test tunnel

The complete test model consists of fuselage, top-mounted inlet, engine centerbody, pressure rakes and conic flow plug as illustrated in Fig. 6. Due to the constraints of wind tunnel blockage and the measurement of internal flow, the wings are not taken into consideration. The test model has a total length of 1000mm and the diameter at the outlet of the inlet, where the measurement of the pressures is made, is 40mm.

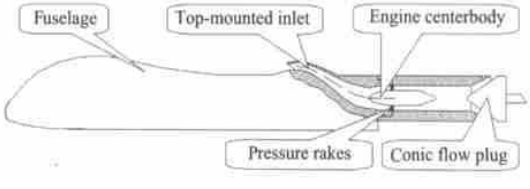

Fig. 6 Sketch of the test model

An eight-leg rake is installed at the outlet of the inlet for measurement of steady total pressure.

Each leg has five probes, providing a total of 40 locations. Four static pressure taps are located on the inner surface of the inlet equally along the circumference and in a plane containing the face of the total pressure probes. The mass flow plug, placed at the model exit and driven by an electric motor, provides flow control for the measurements at different mass flow ratios.

The experimental study is accomplished at NH-1 high speed wind tunnel of NUAA. The Reynolds number of the wind tunnel ranges from 1.2×10^7 to 1.77×10^7. During this test, the free stream Mach number varies from 0.5 to 0.8, angle of attack from -4° to 6° and yaw from 0° to 2°. The maximum blockage of the test section is 4.3% while the inlet model is installed.

3.2 Experimental results

The performance of the inlet is evaluated by the total pressure recovery coefficient (σ) and circular total pressure distortion ($\overline{\Delta\sigma}$). In the following text, the effects of mass flow ratio, free stream Mach number, angle of attack and yaw are illustrated. Contours of total pressure at the outlet of the inlet are also presented.

(1) Total pressure recovery coefficient at different mass flow ratios

In Fig. 7, the total pressure recovery coefficient is plotted as a function of mass flow ratio at 0° angle of attack and yaw. It can be seen that, at first, with the descent of mass flow ratio the recovery coefficient ascends due to the reduction of the friction loss. But when the mass flow ratio goes down further the recovery coefficient tends downwards. The possible reason may be that at low mass flow ratio more low energy flow near the fuselage enters the inlet relative to the total mass flow captured.

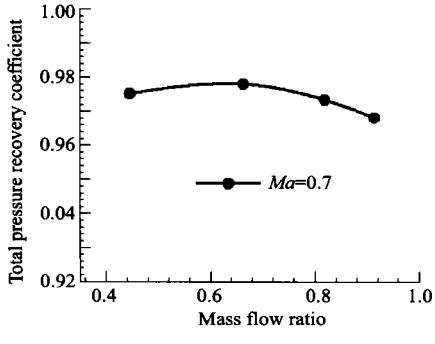

Fig. 7 Total pressure recovery coefficient versus mass flow ratio($\alpha=0^\circ, \beta=0^\circ$)

(2) Effects of free stream Mach number

Fig. 8 shows the variation of total pressure recovery coefficient with free stream Mach number. It can be noted that the recovery coefficient is insensitive to Mach number up to 0.7 and remains above 0.975 stably. This indicates that, despite the negative impact of the bulge and the absence of the boundary diverter, the recovery coefficient of the inlet tested is equivalent to that of conventional S shaped inlet with diverter. However, while the Mach number is greater than 0.7, the recovery coefficient takes on a sharp decline. This trend is probably aroused by a local shock occurring at the back of the bulge, which thickens rapidly the boundary layer and deteriorates the flow condition front of the inlet. It also means that the fuselage configuration like Global Hawk is not suitable for high subsonic flight.

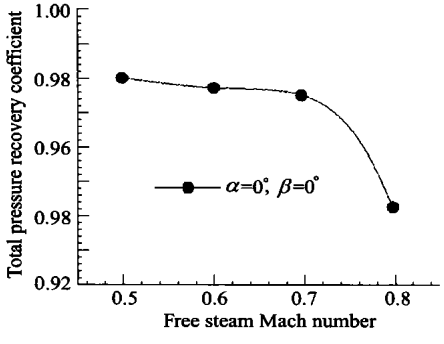

Fig. 8 Total pressure recovery coefficient versus free stream Mach number

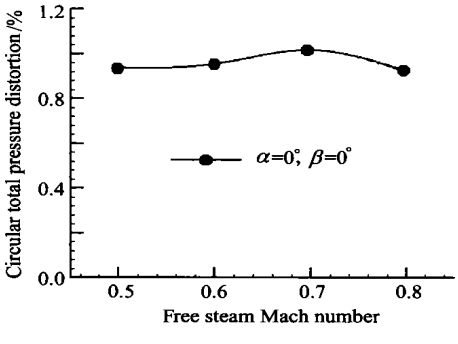

Fig. 9 Circular distortion coefficient versus free stream Mach number

For all test Mach numbers, the circular total pressure distortion keeps below 1.2%, as shown in Fig. 9. It means that the distribution of total pressure losses is nearly constant along circular direction.

(3) Effects of incidence

The model is tested at six angles of attack, of which the range is from -4° to 6°. Fig. 10 and Fig. 11 present the effects of angle of attack on total pressure recovery coeficient and circular total pressure distortion respectively. It can be observed from these two figures that negative angle of attack benefits recovery coefficient and affects distortion slightly, while positive angle of attack affects recovery coefficient slightly and improves distortion obviously. For the case of negative angle, it can be explained as follows: on the one hand, with negative angle of attack rising, the entrance of the inlet is exposed to free stream more and more, resulting in more main flow captured and thereby the increase of total pressure recovery coefficient; on the other hand, the local flow angle of attack at the entrance of the inlet is lower than that of free stream because of the influence of the upper fuselage, which results in a few effect on circular distortion. For the case of positive angle, because the counter-rotating vortex pair developed by the upwash flow around the fore-fuselage sweeps off part of the low energy flow in front of the inlet, the curve of the total pressure recovery goes up a bit from 0° to higher incidence and hence a remarkable drop of circular distortion occurs.

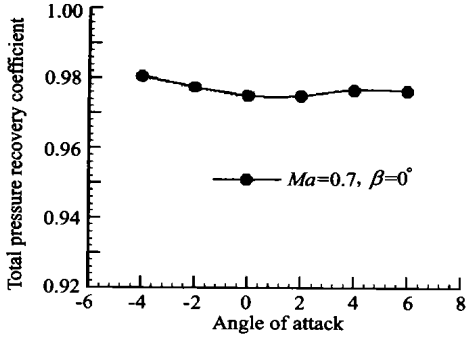

Fig. 10 Total pressure recovery coefficient versus angle of attack

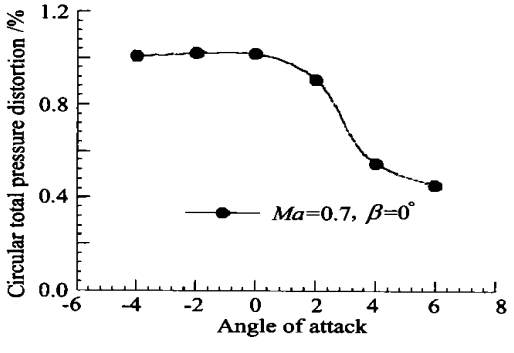

Fig. 11 Circular total pressure distortion coefficient versus angle of attack

(4) Effects of yaw

The effects of yaw on total pressure coefficient and circular total pressure distortion are illustrated in Fig. 12 and Fig. 13. It can be seen that 2° yaw has little effect on recovery coefficient but increases distortion distinctively (still less than 2%). Moreover, with the increase of the Mach number, the performance of the inlet is deteriorating, in particular, at high Mach number, which can be associated with unfavorable flow occurring near the lip at higher Mach number. Consequently, the improvement of performance at yaw will lies on the melioration of cowl lips.

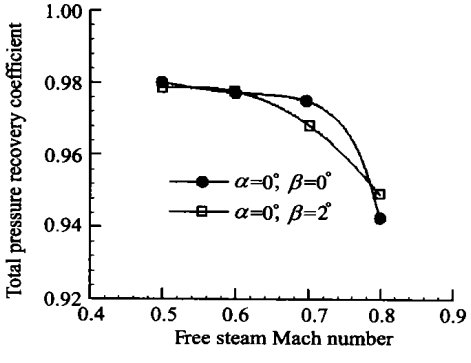

Fig. 12 Effects of yaw on total pressure recovery coefficient

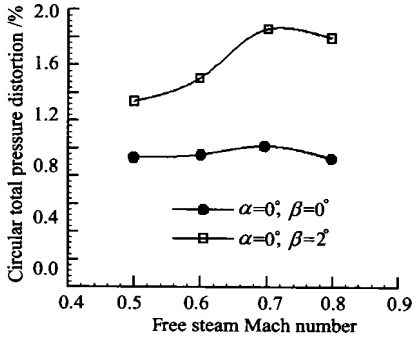

Fig. 13 Effects of yaw on circular distortion coefficient

(5) Total pressure contours

Fig. 14 demonstrates the total pressure distributions at the outlet of the inlet while $Ma = 0.7$, $\alpha = 0°$, $\beta = 0°$. The total pressure contours make a feature of high magnitude and uniform distribution and no obvious low total pressure region exists. All of these suggest that the diverterless technique used in this paper can effectively push the low energy flow away from the inlet, which is validated by CFD results (Fig. 15)[6].

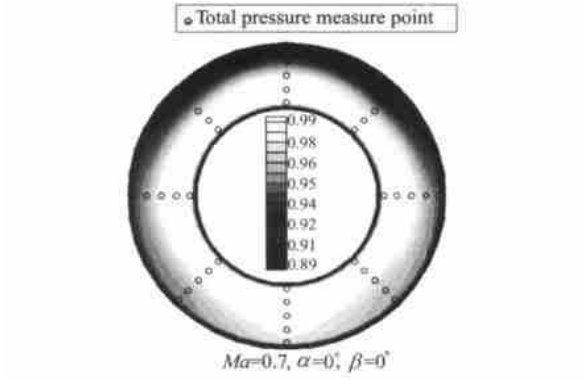

Fig. 14 Contours of total pressure recovery coefficient at the outlet

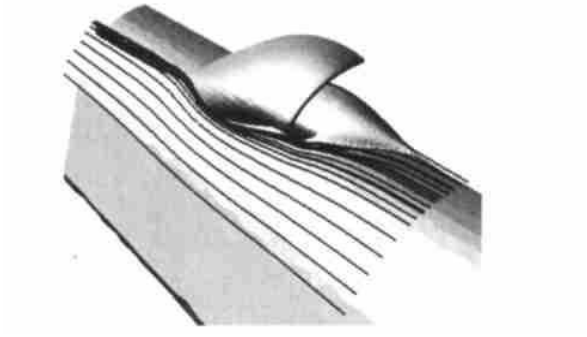

Fig. 15 Streamlines released from points 2mm away from fuselage

4 Conclusions

Design and wind tunnel verification of a top-mounted S shaped inlet utilizing the diverterless technique are reported. During the design process, the integration of the inlet with the fuselage is realized by the utilization of a special inlet section and elimination of conventional diverter, which disposes the whole inlet in the shadow of the bulge improving the drag characteristics and the stealthy performance of the aircraft. Wind tunnel tests indicate that the performance of the inlet advanced here is equivalent to that of conventional S shaped inlet with diverter, so the diverterless technique adopted is successful.

References

[1] Vooren A, Kewenter H, Edefur H. Top mounted air inlet for supersonic & transonic military aircraft [OL]. (2001-05-16) http://www.ave.kth.se/education/msc/courses/4E1232/2001/aero2/TMI_Report.pdf.

[2] Simon P C, Brown D W, Huff R G. Performance of external-compression bump inlet at Mach numbers of 1.5 to 2.0[R]. NACA RM E56L19, 1957.

[3] McFarlan J D. Joint strike fighter diverterless supersonic inlet [OL], (2000-11-15). http://www.codeonemagzine.com/archieves/2000/articles/july_00/divertless_1.html.

[4] Lee C C, Boekicker C. Subsonic diffuser design and performance for advanced fighter aircraft [R], AIAA-85-3073, 1985.

[5] Richard J R. An investigation of several NACA-series inlets at Mach number from 0.4 to 1.29 for mass-flow ratio near 1.0 [R]. NASA TM-X-3324, 1975.

[6] 谭慧俊, 郭荣伟. 背负式无隔道进气道的方案设计与性能研究[R]. 南京航空航天大学科技报告, R0202018, 2002.
Tan H J, Guo R W. Design and performance study of a top-mounted diverterless inlet [R]. Technical Report of NUAA, R0202018, 2002. (in Chinese)

Biography:

TAN Hui-jun Born in 1975, he received Ph. D. degree from Nanjing University of Aeronautical and Astronautics in 2003, and then became a teacher there. His research interests focus on CFD and experimental investigations of internal flow. Tel: (025) 84892203-2415, E-mail: tanzi109@263.net